



Contents lists available at ScienceDirect



# Catalysis Today

journal homepage: [www.elsevier.com/locate/cattod](http://www.elsevier.com/locate/cattod)

## Epoxidation of olefins with oxygen/isobutyraldehyde over transition-metal-substituted phosphomolybdic acid on SBA-15

Xiaojing Song<sup>a</sup>, Wanchun Zhu<sup>a</sup>, Kaige Li<sup>a</sup>, Jing Wang<sup>a</sup>, Huiling Niu<sup>a</sup>, Hongcheng Gao<sup>a</sup>, Wenxiu Gao<sup>a</sup>, Wenxiang Zhang<sup>a</sup>, Jihong Yu<sup>b</sup>, Mingjun Jia<sup>a,\*</sup>

<sup>a</sup> Key Laboratory of Surface and Interface Chemistry of Jilin Province, College of Chemistry, Jilin University, 130021 Changchun, China

<sup>b</sup> State Key Laboratory of Inorganic Synthesis and Preparative Chemistry, College of Chemistry, Jilin University, Changchun 130012, China

### ARTICLE INFO

#### Article history:

Received 28 February 2015

Received in revised form 27 April 2015

Accepted 28 April 2015

Available online xxx

#### Keywords:

Transition metal

Phosphomolybdic acid

Olefin

SBA-15

Epoxidation

### ABSTRACT

A series of polyoxometalate-based heterogeneous catalysts were prepared by immobilized transition metal mono-substituted phosphomolybdic acids ( $\text{PMo}_{11}\text{M}$ ,  $\text{M}=\text{Fe, Co or Cu}$ ) or unsubstituted phosphomolybdic acid ( $\text{PMo}_{12}$ ) on amino-functionalized SBA-15. A variety of characterization results demonstrated that the  $\text{PMo}_{11}\text{M}$  units are uniformly dispersed on the surface or in the channels of mesoporous SBA-15. The catalytic properties of these hybrid materials (denoted as  $\text{PMo}_{11}\text{M}/\text{SBA}$  or  $\text{PMo}_{12}/\text{SBA}$ ) were investigated in the epoxidation of olefins with molecular oxygen as oxidant and isobutyraldehyde as co-reactant. It has been found that  $\text{PMo}_{11}\text{Co}/\text{SBA}$  and  $\text{PMo}_{11}\text{Cu}/\text{SBA}$  are catalytically active for the epoxidation of cyclooctene with acetonitrile as solvent, while  $\text{PMo}_{11}\text{Fe}/\text{SBA}$  and  $\text{PMo}_{12}/\text{SBA}$  are nearly inactive under the same reaction conditions. Moreover, the relatively active  $\text{PMo}_{11}\text{Co}/\text{SBA}$  catalyst could also efficiently convert cyclohexene and 1-octene to the corresponding epoxides, and its catalytic activity was solvent dependent. Using suitable solvent like acetonitrile could efficiently inhibit the deactivation of the catalyst, thus bringing excellent stability and recyclability for the  $\text{PMo}_{11}\text{Co}/\text{SBA}$  catalyst.

© 2015 Elsevier B.V. All rights reserved.

## 1. Introduction

The epoxidation of olefins is an industrially important process since epoxides are widely used as key intermediates in organic synthesis [1–3]. Recently, considerable interests have been drawn on studying the aerobic epoxidation of olefins for developing more efficient and environmentally benign route [4–7]. It was reported that aerobic epoxidation of olefins in solution can be efficiently achieved under quite mild conditions over some transition metal complexes by using molecular oxygen as oxidant and aliphatic aldehyde as co-reactant, which is the so-called “Mukaiyama” procedure [8–13]. Although the usage of co-reactant aldehyde is undesirable, the Mukaiyama method is still worthy of studying for its great advantages, such as very mild operation conditions (low temperatures, atmospheric pressure), high epoxide selectivity, low cost and environmental-friendly nature of the oxidant [11–13].

In general, Mukaiyama epoxidation could be catalyzed by using some homogeneous transition metal complexes like  $\beta$ -diketonate complexes, Schiff's base complexes, metal cyclam complexes and metalloporphyrins complexes [8–13]. For overcoming the

separation and recycling problems of the homogeneous catalysts, recent efforts were mainly focused on preparing efficient heterogeneous catalysts [14–23]. Representative catalysts include various transition metal complexes supported on porous materials, Co-containing zeolitic imidazolate framework material, Cu/Ga-based metal-organic framework (MOF) and so on [14–23]. However, in most cases, either the catalytic activity or the selectivity to epoxide of these heterogeneous catalysts is still not very satisfied. Moreover, leaching of active species during the reaction course is commonly occurred. Therefore, it is still an attractive subject to develop more efficient heterogeneous catalysts for Mukaiyama epoxidation.

As an important catalyst system in selective oxidation, polyoxometalate (POM) including various transition metal-substituted phosphomolybdate, has shown numerous advantageous properties, such as thermodynamic stability to oxidation, hydrostability, tunability of redox and acid properties [24–30]. By immobilizing various POMs on different supports like oxides, zeolites, carbons etc., some highly efficient POM-based heterogeneous catalysts have already been obtained for important catalytic oxidation reactions [31–37]. Particularly, it was reported that a few supported POM catalysts can also catalyze the aerobic epoxidation of olefins in the presence of aldehydes. For instance, Johnson and Stein [24] reported amine-modified silica supported Co- and Zn-substituted phosphotungstates or silicotungstates are

\* Corresponding author. Tel.: +86 431 85155390; fax: +86 431 85168420.

E-mail address: [jiam@jlu.edu.cn](mailto:jiam@jlu.edu.cn) (M. Jia).

active catalysts for the aerobic epoxidation of cyclohexene in the presence of isobutyraldehyde (IBA). Kholdeeva and coauthors [25] found that amine-modified mesoporous silicate supported  $[Bu_4N]_4H[PW_{11}Co(H_2O)_{39}]$  can efficiently catalyze the aerobic oxidation of  $\alpha$ -pinene to epoxide with IBA as co-reactant. Concerning the diversity of POM in composition, structure and property, one can expect that there will be very broad space for developing more efficient heterogeneous POM-based catalysts for Mukaiyama epoxidation reactions.

Previously, our group has already carried out some works on preparing various POM-based heterogeneous catalysts for olefin epoxidation with *tert*-butyl hydroperoxide or  $H_2O_2$  as oxidants [38–41]. As a continuation of these works, we here tried to immobilize a series of transition metal-substituted phosphomolybdic acids on to  $NH_2$ -modified SBA-15 (denoted as  $PMo_{11}M/SBA$ , M = Co, Cu, Fe) and to test their catalytic performance for the aerobic epoxidation of olefins in the presence of IBA. It was found that supported Co-substituted phosphomolybdate catalyst can efficiently catalyze a variety of olefins to corresponding epoxides, and can also be easily recycled for a few times without obvious loss in its catalytic activity.

## 2. Experimental

### 2.1. Catalyst preparation

#### 2.1.1. Preparation of transition metal mon-substituted phosphomolybdc acids

Transition metal (Fe, Co, Cu) mon-substituted phosphomolybdc acids were prepared according to a literature procedure for the preparation of molybdoavanadophosphoric acids [42].  $Na_2HPO_4 \cdot 12H_2O$  (0.01 mol) was dissolved in 20 ml of water and mixed with nitrates of corresponding metal (0.01 mol) that had been dissolved by boiling in 20 ml of water. The mixture was cooled and acidified with 1.0 ml of concentrated sulfuric acid. To this mixture a solution of 0.11 mol of  $Na_2MoO_4 \cdot 2H_2O$  dissolved in 40 ml of water was added, large amount of flocculent precipitate appeared. After that, some amount of concentrated sulfuric acid was added slowly with vigorous stirring until it turned to a clear solution. The heteropoly acid was then extracted with 400 ml of ethyl ether after the water solution was cooled. In this extraction, the heteropoly etherate was present as a bottom layer. After separation, a stream of air was passed through the heteropoly etherate layer to free it of ether. The green-yellow solid that remained was dissolved in 50 ml of water, concentrated to the first appearance of crystals in a vacuum desiccator over concentrated sulfuric acid, and then allowed to crystallize further. Finally,  $H_6PMo_{11}FeO_{40} \cdot xH_2O$ ,  $H_7PMo_{11}CoO_{40} \cdot xH_2O$  and  $H_7PMo_{11}CuO_{40} \cdot xH_2O$  were obtained, and denoted as  $PMo_{11}M$  (M = Fe, Co, Cu) hereafter. The calculated analytic values (at.%) presented below, all the relative errors were within the scope permitted:  $PMo_{11}Fe$  [P (7.19%) Mo (85.39%) Fe (7.42%)];  $PMo_{11}Co$  [P (7.32%) Mo (81.45%) Co (6.98%)];  $PMo_{11}Cu$  [P (8.26%) Mo (85.45%) Cu (7.95%)].

#### 2.1.2. Preparation of amine-functionalized of SBA-15

SBA-15 was prepared according to the literature method [43]. Functionalization of SBA-15 was conducted with schrank

techniques [44]. About 1.0 g SBA-15 was treated at 150 °C for 2 h under vacuum. About 30 ml dry toluene was added into the flask quickly, then 2 mmol 3-aminopropyltriethoxysilane (APTES) was added into the suspension under  $N_2$  protection and refluxed at 110 °C for 24 h. Afterwards, the solid was filtered and washed with toluene and anhydrous ethanol for several times. Finally, the solid was extracted using a Soxhlet 24 h with dichloroethane and dried in vacuum overnight. The resulting material was denoted as  $NH_2$ -SBA-15.

#### 2.1.3. Immobilization of $PMo_{11}M$ (M = Fe, Co, Cu) on $NH_2$ -SBA-15

A certain quality of  $NH_2$ -SBA-15 was added into a 30 ml methanol solution containing some amount of  $PMo_{11}M$  (M = Fe, Co, Cu), and refluxed for 6 h. It was then filtered and Soxhleted for 24 h with methanol and dried in vacuum at 80 °C. The resulting product is designated as  $PMo_{11}M/SBA$  (M = Fe, Co, Cu). For comparison, a reference catalyst of  $PMo_{12}/SBA$  was also prepared by immobilizing commercial phosphomolybdc acids ( $PMo_{12}$ ) on  $NH_2$ -SBA-15. The loading of  $PMo_{11}M$  (or  $PMo_{12}$ ) in the supported catalysts was determined by inductively coupled plasma-optical emission spectroscopy (ICP-AES), and the concreted values are given in Table 1.

### 2.2. Catalysts characterization

Powder X-ray diffraction (XRD) patterns were recorded on a Shimadzu XRD-6000 diffractometer (40 kV, 30 mA), using Ni-filtered  $Cu K\alpha$  radiation.

FT-IR spectra were recorded on a Nicolet AVATAR 370 DTGS spectrometer in the range 4000–500  $cm^{-1}$ .

$N_2$  adsorption/desorption isotherms were measured at 77 K using a Micromeritics ASAP 2010 N analyzer. Samples were degassed at 150 °C for 8 h before measurements. Specific surface areas were calculated using BET model. Pore volumes are estimated at a relative pressure of 0.94 ( $P/P_0$ ), assuming full surface saturation with nitrogen. Pore size distributions are evaluated from desorption branches of the nitrogen isotherms using the BJH model.

Transmission electron microscopy (TEM) images were taken with a H8100-IV electron microscope with an energy-dispersive X-ray spectroscopy (EDX) operating at 200 kV. The samples were suspended in ethanol by sonication and then picked up on a Cu grid covered with a carbon film.

XPS measurements were made on a VGESCA LAB MK-II X-ray electron spectrometer using  $Al K\alpha$  radiation.

### 2.3. Catalyst test

The catalytic oxidation reaction was carried out in a 50 ml three-necked bottle equipped with a stirring bar, reflux condenser, and gas supply. Solvent, olefin, IBA and catalyst were added into the flask respectively, and the whole device was placed in a temperature-controlled oil bath. To commence the reaction, oxygen was passed through the reactor at a flow rate of 10 ml/min<sup>-1</sup> under atmosphere. The oxidation products of the reaction were analyzed and quantified by Shimadzu GC-8A gas chromatograph with HP-5 capillary column.

**Table 1**

Texture parameters of SBA-15,  $PMo_{12}/SBA$  and  $PMo_{11}M/SBA$  materials.

Catalyst	$PMo_{11}M$ (mmol/g)	Surface Area ( $m^2/g$ )	Pore volume ( $cm^3/g$ )	Average pore diameter (nm)
SBA-15	–	794	1.48	7.2
$PMo_{12}/SBA$	0.093	265	0.53	5.7
$PMo_{11}Fe/SBA$	0.105	244	0.46	5.2
$PMo_{11}Co/SBA$	0.101	231	0.41	5.8
$PMo_{11}Cu/SBA$	0.066	316	0.64	4.9

### 3. Results and discussion

#### 3.1. Catalyst characterization

The XRD patterns of  $\text{PMo}_{11}\text{M}/\text{SBA}$  ( $\text{M} = \text{Fe}, \text{Co}, \text{Cu}$ ) catalysts and unsupported  $\text{PMo}_{11}\text{M}$  are shown in Fig. 1. Unsupported  $\text{PMo}_{11}\text{M}$  samples exhibit characteristic XRD peaks at  $2\theta = 15$  and  $30^\circ$  (Fig. 1A). Compared with  $\text{PMo}_{12}$ , the slight changes in  $2\theta$  values of  $\text{PMo}_{11}\text{M}$  ( $\text{M} = \text{Fe}, \text{Co}, \text{Cu}$ ) should be related to the partial substitution of Mo by M, which are consistent to the early literature results [45]. The low-angle XRD patterns of  $\text{PMo}_{11}\text{M}/\text{SBA}$  catalysts are shown in Fig. 1B. SBA-15 exhibits an intense peak assigned to reflections at  $(100)$  and two low-intensity peaks at  $(110)$  and  $(200)$ , indicating a significant degree of long-range ordering in the structure and a well-formed hexagonal lattice. The  $\text{NH}_2\text{-SBA-15}$  shows quite similar diffraction peaks to SBA-15, although slight decrease in intensity can be observed. For  $\text{PMo}_{11}\text{M}/\text{SBA}$  and  $\text{PMo}_{12}/\text{SBA}$ , significant decrease in diffraction peak intensity is detected, indicating that POM anions have been introduced into the channels of SBA-15. From wide-angle XRD patterns of supported catalysts (inset of Fig. 1B), all hybrid materials exhibit only one very broad peak, which is a characteristic of amorphous materials. The absence

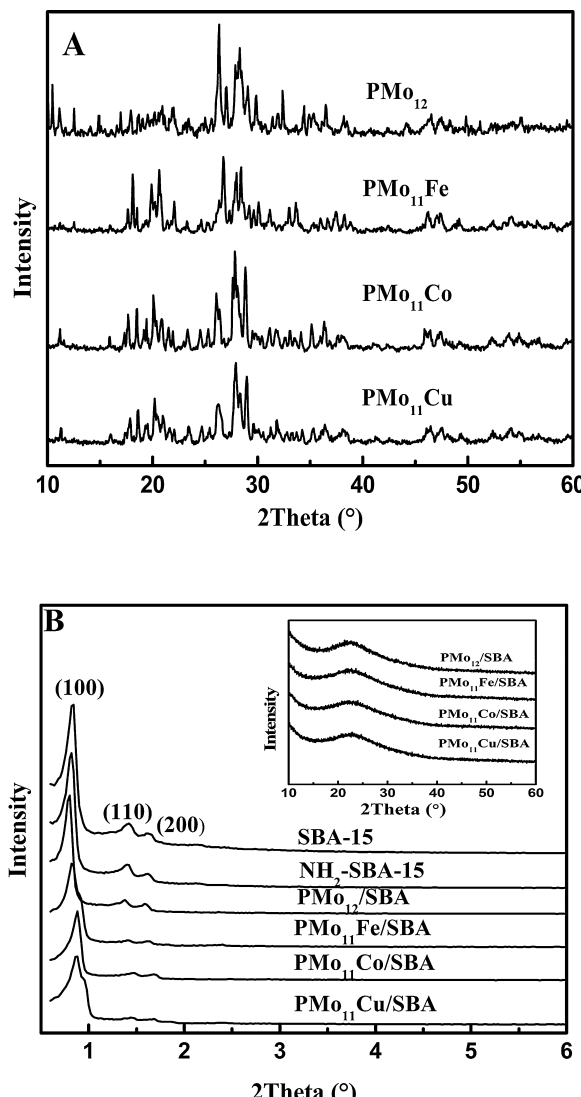


Fig. 1. XRD patterns of (A) unsupported  $\text{PMo}_{11}\text{M}$  and (B) supported  $\text{PMo}_{11}\text{M}/\text{SBA}$  ( $\text{M} = \text{Mo, Fe, Co, Cu}$ ) catalysts.

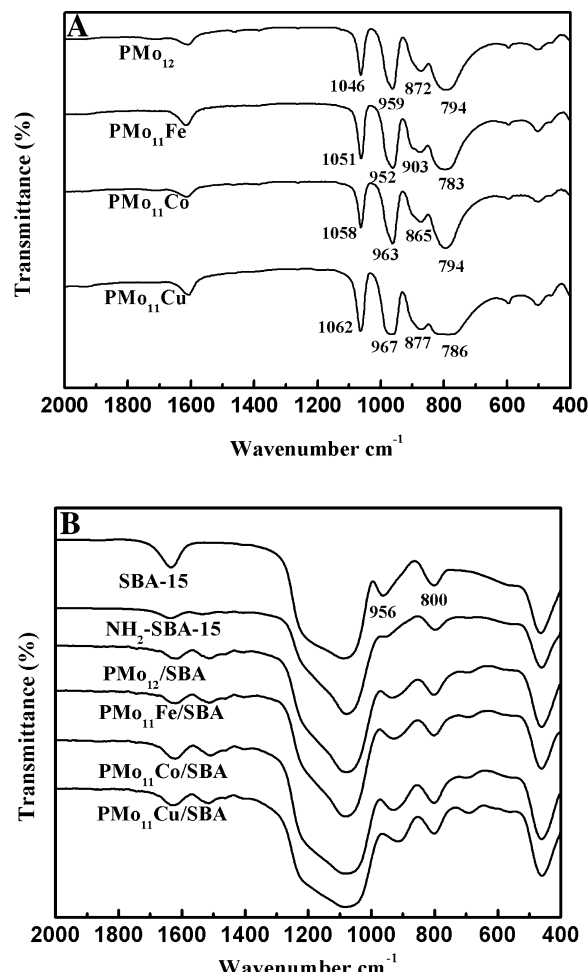
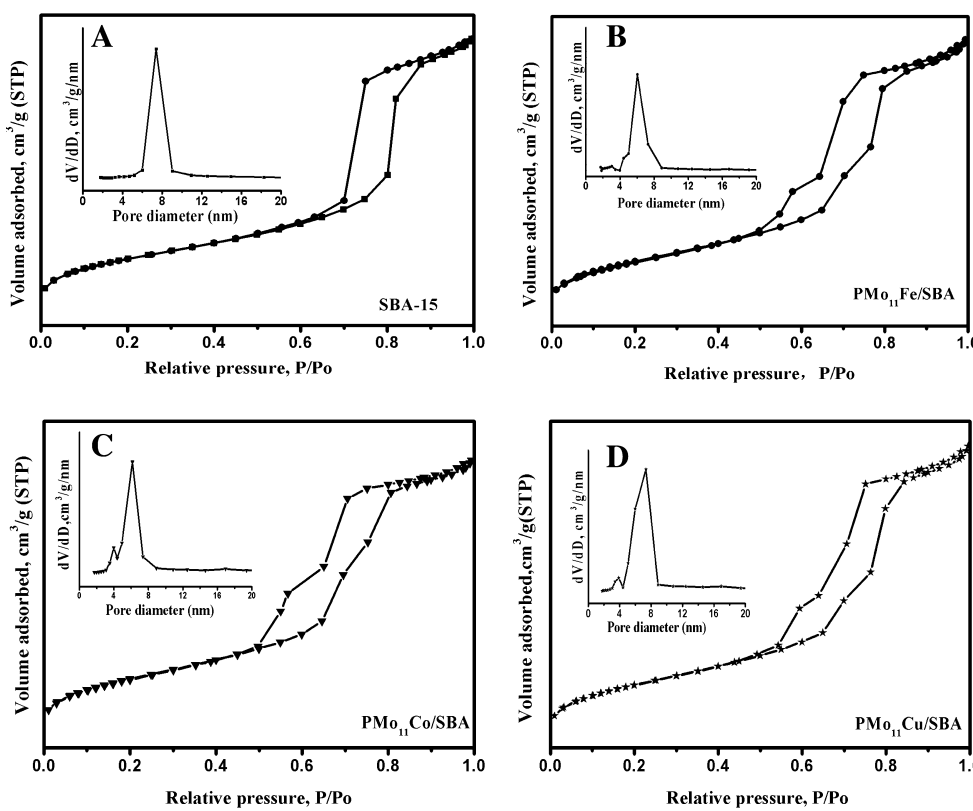


Fig. 2. FT-IR spectra of unsupported  $\text{PMo}_{11}\text{M}$  and  $\text{PMo}_{12}$ , as well as the SBA-15 supported POM catalysts.

of diffraction peaks of crystalline POM in the wide-angle region, suggests that the introduced POM units are highly dispersed on the surface and/or in the channel of the SBA-15 supports support [31,46].

The FT-IR spectra of unsupported  $\text{PMo}_{11}\text{M}$  and  $\text{PMo}_{12}$ , as well as the SBA-15 supported POM catalysts are shown in Fig. 2. Characteristic bands of  $\text{PMo}_{12}$  appeared at  $1046\text{ cm}^{-1}$ ,  $959\text{ cm}^{-1}$ ,  $872\text{ cm}^{-1}$  and  $794\text{ cm}^{-1}$  can be assigned to the vibrations of  $\text{P}-\text{O}$ ,  $\text{Mo}=\text{O}$ ,  $\text{Mo}-\text{O}_\text{b}-\text{Mo}$  and  $\text{Mo}-\text{O}_\text{c}-\text{Mo}$  bonds, respectively [45]. For the three  $\text{PMo}_{11}\text{M}$  samples, the corresponding vibration bands shift slightly, which is an indication of the distortion induced by the partial replacement of Mo by M ( $\text{M} = \text{Fe}, \text{Co}, \text{Cu}$ ). As shown in Fig. 2B, SBA-15 and  $\text{NH}_2\text{-SBA-15}$  exhibit a few strong absorbed bands in the region of  $2000\text{--}400\text{ cm}^{-1}$ , which can be mainly assigned to the characteristic vibrations of  $\text{Si}-\text{O}-\text{Si}$  bonds. The spectra of the  $\text{PMo}_{11}\text{M}/\text{SBA}$  catalysts are quite similar to that of SBA-15 support. No obvious characteristic peaks of POM units can be distinguished in the spectra, which should be due to the overlap with the absorbed peaks of SBA-15 support.

The nitrogen adsorption-desorption isotherms of SBA-15 and  $\text{PMo}_{11}\text{M}/\text{SBA}$  ( $\text{M} = \text{Fe}, \text{Co}, \text{Cu}$ ) are shown in Fig. 3. All the samples displayed a type IV isotherm according to the IUPAC classification. The appearance of H1 hysteresis loop is a characteristic of mesoporous materials and the capillary condensation occurs at relative pressure ( $P/P_0$ ) of  $0.45\text{--}0.85$ . Compared with the support SBA-15, there are pronounced decrease of the BET surface area, the pore volume, and the pore size in the SBA-15 supported POM catalysts



**Fig. 3.**  $\text{N}_2$  adsorption-desorption isotherms and pore size distribution of materials (A) SBA-15, (B)  $\text{PMo}_{11}\text{Fe}/\text{SBA}$ , (C)  $\text{PMo}_{11}\text{Co}/\text{SBA}$ , and (D)  $\text{PMo}_{11}\text{Cu}/\text{SBA}$ .

(as shown in Table 1), which could be attributed to the introduction of  $\text{PMo}_{11}\text{M}$ .

TEM images of the SBA-15,  $\text{NH}_2\text{-SBA-15}$ ,  $\text{PMo}_{11}\text{Fe}/\text{SBA}$  and  $\text{PMo}_{11}\text{Co}/\text{SBA}$  are shown in Fig. 4. The results confirm the characteristic pore dimensions and channel structures of the support materials, and provide strong evidence that the mesoporous structure of SBA-15 supports remains intact after the introduction of POM units.

XPS spectra of Mo 3d for  $\text{PMo}_{12}/\text{SBA}$  and  $\text{PMo}_{11}\text{M}/\text{SBA}$  ( $\text{M} = \text{Fe}, \text{Co}, \text{Cu}$ ) are shown in Fig. 5.  $\text{PMo}_{12}/\text{SBA}$  displays characteristic 236.3 and 233.2 eV, which are attributed to  $\text{Mo(VI)} 3\text{d}_{3/2}$  and  $\text{Mo(VI)} 3\text{d}_{5/2}$ , respectively [47]. For  $\text{PMo}_{11}\text{Fe}/\text{SBA}$  and  $\text{PMo}_{11}\text{Co}/\text{SBA}$ , there are no obvious changes in the values of the binding energy (BE) of Mo species in comparison with that of  $\text{PMo}_{12}/\text{SBA}$ . As for  $\text{PMo}_{11}\text{Cu}/\text{SBA}$ , slightly lower binding energy of Mo species could be detected. Apparently, the chemical states of Mo species in all the  $\text{PMo}_{11}\text{M}/\text{SBA}$  catalysts are quite similar. This might be due to the fact that only a small portion of Mo species in the POM clusters are substituted by transition metal ions.

### 3.2. Catalytic results

The catalytic properties of  $\text{PMo}_{11}\text{M}/\text{SBA}$  ( $\text{M} = \text{Fe}, \text{Co}, \text{Cu}$ ) and  $\text{PMo}_{12}/\text{SBA}$  catalysts were investigated for the aerobic epoxidation of olefins with  $\text{CH}_3\text{CN}$  or  $\text{CHCl}_3$  as solvent and isobutyraldehyde as co-reactant (Table 2). When using acetonitrile ( $\text{CH}_3\text{CN}$ ) as solvent,  $\text{PMo}_{11}\text{Co}/\text{SBA}$  gives 98% of conversion of cyclooctene after 3 h and performs the highest catalytic activity among the test catalysts. Catalyst  $\text{PMo}_{11}\text{Cu}/\text{SBA}$  shows a lower activity, 76.9% of conversion is obtained after 3 h reaction. Notably, both  $\text{PMo}_{11}\text{Fe}/\text{SBA}$  and  $\text{PMo}_{12}/\text{SBA}$  are nearly inactive for the aerobic epoxidation of cyclooctene, and no obvious conversion of cyclooctene can be detected under the test conditions. In the case of using chloroform ( $\text{CHCl}_3$ ) as solvent, relatively low conversion of cyclooctene

(64% after 3 h) is achieved over the  $\text{PMo}_{11}\text{Co}/\text{SBA}$  catalyst, indicating the solvent-dependent of this epoxidation reaction. Besides, all catalysts exhibit very high selectivity to epoxide (>99%), and no detectable side products are observed under the test conditions.

The recycling experiments of  $\text{PMo}_{11}\text{Co}/\text{SBA}$  for the aerobic epoxidation of cyclooctene were carried out with  $\text{CH}_3\text{CN}$  as the solvent. After each experiment, the filtrate catalyst was washed with  $\text{CH}_3\text{CN}$  and dried under vacuum, then reused without further treatment. As shown in Fig. 6,  $\text{PMo}_{11}\text{Co}/\text{SBA}$  shows very good recyclability, no obvious loss in activity could be observed with the increase of recycle numbers. In addition, a leaching test was conducted to verify the heterogeneity of the catalytic process. It has been found that there is no significant increase of conversion of cyclooctene after removing the  $\text{PMo}_{11}\text{Co}/\text{SBA}$  catalyst by filtration at reaction temperature, indicating the truly heterogeneous catalysis of the catalyst.

Previously, mechanistic studies on the Mukaiyama epoxidation of olefins have revealed that this reaction proceeds mainly through a radical pathway [15,24]. The active epoxidizing species are acyl peroxy radicals, which are produced from the decomposition of acyl peroxy acid (formed from the autoxidation of aldehyde) over

**Table 2**

Catalytic properties of  $\text{PMo}_{11}\text{M}/\text{SBA}$  ( $\text{M} = \text{Fe}, \text{Co}, \text{Cu}$ ) and  $\text{PMo}_{12}/\text{SBA}$  in the aerobic epoxidation of cyclooctene with IBA as co-reactant.<sup>a</sup>

Catalyst	Solvent	Time (h)	Conversion (%)	Selectivity (%)
$\text{PMo}_{11}\text{Co}/\text{SBA}$	$\text{CH}_3\text{CN}$	1	43	>99
	$\text{CH}_3\text{CN}$	3	98	
	$\text{CHCl}_3$	1	15	>99
	$\text{CHCl}_3$	3	64	
$\text{PMo}_{11}\text{Cu}/\text{SBA}$	$\text{CH}_3\text{CN}$	1	6	>99
	$\text{CH}_3\text{CN}$	3	76	
$\text{PMo}_{11}\text{Fe}/\text{SBA}$	$\text{CH}_3\text{CN}$	3	<1	–
$\text{PMo}_{12}/\text{SBA}$	$\text{CH}_3\text{CN}$	3	<1	–

<sup>a</sup> Reaction conditions: catalyst 10 mg, cyclooctene 1.0 mmol,  $\text{CH}_3\text{CN}$  10 ml, flow of air 10 ml/min, IBA 2.0 mmol, reaction temperature 40 °C.

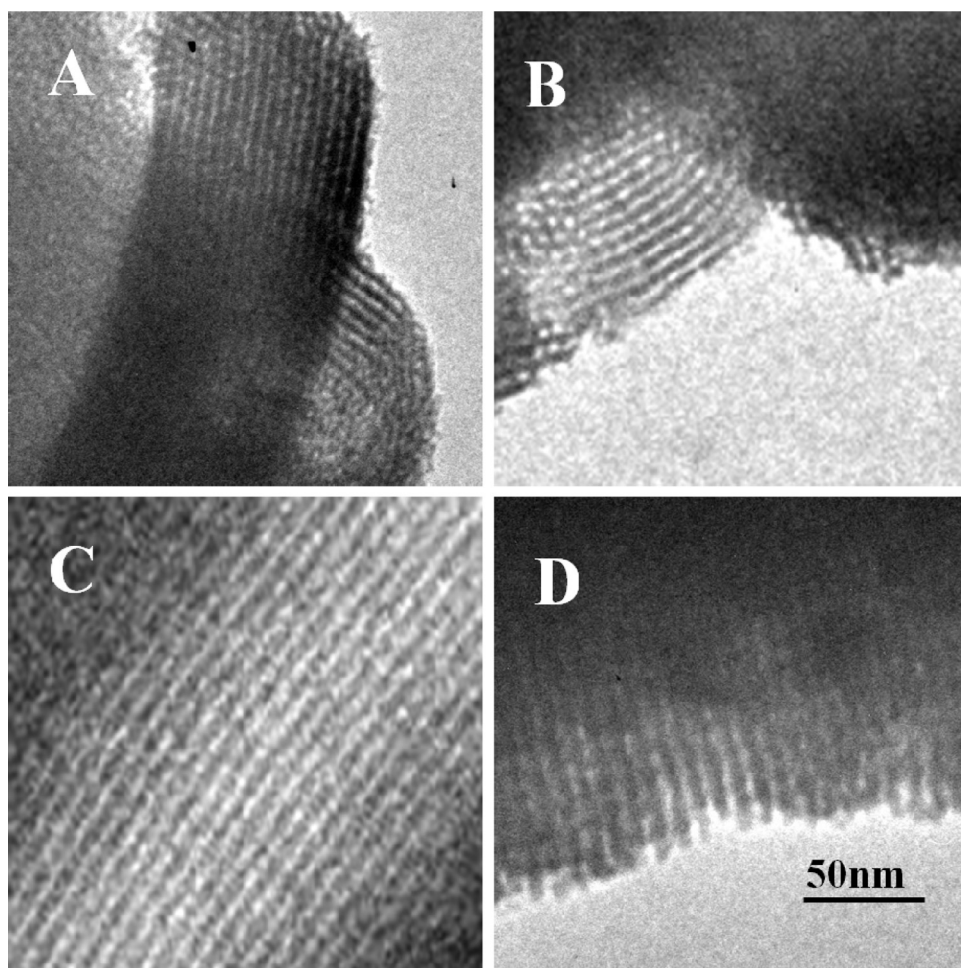


**Fig. 4.** TEM for (A) SBA-15, (B) NH<sub>2</sub>-SBA-15, (C) PMo<sub>11</sub>Fe/SBA, and (D) PMo<sub>11</sub>Co/SBA.

catalyst. Therefore, the difference in catalytic activity of the different PMo<sub>11</sub>M/SBA (M = Fe, Co, Cu) catalysts should originate from the different activation ability of the transition metal cations to form acyl peroxy radicals. Besides, their catalytic properties may also reflect the ability of metal cations against complex reagents (e.g., poisoned by acyl peroxy acid). The relatively high activity of Co-based catalyst (PMo<sub>11</sub>Co/SBA) suggests that Co ions should

be the main active sites for decomposing acyl peroxy acids to form acyl peroxy radicals. On other hand, the very poor activity of PMo<sub>11</sub>Fe/SBA catalyst may be indicative that Fe species can strongly coordinate with acyl peroxy acid to form the stable complexes that inhibited the further oxidation of olefins [48].

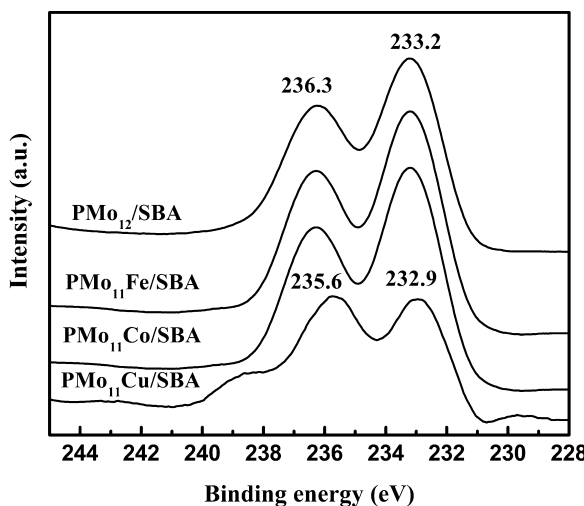


**Fig. 5.** XPS spectra of Mo (3d<sub>3/2</sub>) and Mo (3d<sub>5/2</sub>) for PMo<sub>11</sub>M/SBA catalysts.

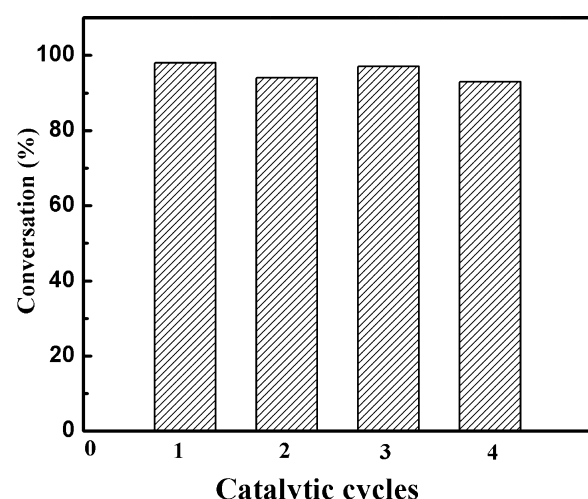


**Fig. 6.** Recycling experiments of PMo<sub>11</sub>Co/SBA catalyst in the aerobic oxidation of cyclooctene. Reaction conditions: catalyst 10 mg, cyclooctene 1.0 mmol, CH<sub>3</sub>CN 10 ml, flow of air 10 ml/min, IBA 2.0 mmol, reaction temperature 40 °C, and reaction time 3 h.

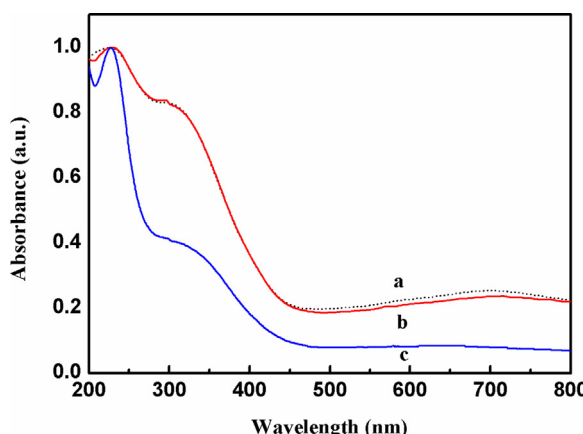


**Fig. 7.** DRS-UV spectra of  $\text{PMo}_{11}\text{Co}/\text{SBA}$  catalyst (a) fresh one, (b) treated with 0.3 M IBAc in  $\text{CH}_3\text{CN}$ , and (c) treated with 0.3 M IBAc in  $\text{CHCl}_3$ .

In addition, our results have shown that changing the solvents could also significantly influence the catalytic activity of  $\text{PMo}_{11}\text{Co}/\text{SBA}$  catalyst. Much lower activity in  $\text{CHCl}_3$  is obtained as compared to  $\text{CH}_3\text{CN}$ . In order to explain this phenomenon, DRS-UV-vis study was carried out to characterize the  $\text{PMo}_{11}\text{Co}/\text{SBA}$  catalysts treated either by isobutyric acid (IBAc)/ $\text{CH}_3\text{CN}$  or by IBAc/ $\text{CHCl}_3$ , following a literature reported method [25]. As shown in Fig. 7, the position of the d-d transition bands of Co species in the IBAc/ $\text{CH}_3\text{CN}$  treated catalyst is quite similar to the fresh catalyst, whereas the bands position for the IBAc/ $\text{CHCl}_3$  treated catalyst shifts toward higher wavelength. Additional experimental results

suggest that the IBAc/ $\text{CHCl}_3$  treated  $\text{PMo}_{11}\text{Co}/\text{SBA}$  catalyst is nearly inactive for the aerobic epoxidation of cyclooctene with  $\text{CHCl}_3$  as solvent, while its activity can be recovered after the catalyst is washed with  $\text{CH}_3\text{CN}$  and dried in the vacuum. These results suggest that IBAc could strongly interact with Co species in the presence of  $\text{CHCl}_3$  solvent, which might be the main reason for decreasing the catalytic activity of  $\text{PMo}_{11}\text{Co}/\text{SBA}$ . When using  $\text{CH}_3\text{CN}$  as solvent, the negative effect of IBAc on catalytic activity can be overcome, possibly due to the fact that  $\text{CH}_3\text{CN}$  could act as a competitive ligand to coordinate with Co ions during the reaction course, thus avoiding the deactivation/poison caused by strong coordination role of IBAc [49].

The catalytic properties of  $\text{PMo}_{11}\text{Co}/\text{SBA}$  catalysts were also investigated in the epoxidation of cyclohexene with  $\text{O}_2/\text{IBA}$ , since cyclohexene is a good substrate to study the issue of selectivity control for the POM-based catalysts [24,41]. As shown in Table 3, the aerobic epoxidation of cyclohexene in the presence of IBA easily occurs even without addition of catalysts, and 17% conversion of cyclohexene is obtained with nearly 100% selectivity of epoxide in the blank test. Among the three supported POM catalysts, the reactivity follows the order of  $\text{PMo}_{11}\text{Co}/\text{SBA} > \text{PMo}_{11}\text{Cu}/\text{SBA} > \text{PMo}_{11}\text{Fe}/\text{SBA}$ , which is in agreement with the active order for cyclooctene epoxidation. In fact, the catalytic activity of  $\text{PMo}_{11}\text{Fe}/\text{SBA}$  catalyst is neglectable, since it gives almost the same conversion as the blank reaction. The activities of  $\text{PMo}_{11}\text{Co}/\text{SBA}$  and  $\text{PMo}_{11}\text{Cu}/\text{SBA}$  are comparable with other heterogeneous catalysts reported in literatures (the representative results are also given in Table 3). In addition, small amount of 2-cyclohexene-1-one can be detected over the two  $\text{PMo}_{11}\text{M}/\text{SBA}$  catalysts, whereas the epoxide product is still the main product

**Table 3**  
Comparison of the catalytic properties of  $\text{PMo}_{11}\text{M}/\text{SBA}$  catalysts with other literature reported catalysts for the aerobic epoxidation cyclohexene with IBA as co-reagent.<sup>a</sup>

Catalyst	Temp (°C)	Time (h)	Con (%)	Selectivity (%)			Related work
				Epoxide	one <sup>b</sup>	ol or diol <sup>c</sup>	
None (blank)	40	4	17	>99	nd	nd	This work
$\text{PMo}_{11}\text{Co}/\text{SBA}$	40	4	81	90	10	nd	This work
$\text{PMo}_{11}\text{Cu}/\text{SBA}$	40	4	70	90	10	nd	This work
$\text{PMo}_{11}\text{Fe}/\text{SBA}$	40	4	18	>99	nd	nd	This work
Co/ZIF <sup>d</sup>	30	3	100	70	30	nd	[14]
CoPO <sub>4</sub> -MOF <sup>d</sup>	60	16	93	68	nd	32	[19]
CoTE3PyP/MT <sup>d</sup>	25	9	76	87	13	nd	[21]
Cu@COMOC-4 <sup>d</sup>	40	7	49	89	4.3	6.5	[23]

<sup>a</sup> Reaction conditions in this work: catalyst 10 mg, cyclohexene 1.0 mmol, IBA 2.0 mmol, 10 ml of  $\text{CH}_3\text{CN}$ ,  $\text{O}_2$  1 atm.

<sup>b</sup> 2-Cyclohexen-1-one.

<sup>c</sup> 2-Cyclohexen-1-ol or 1,2-cyclohexanediol.

<sup>d</sup> See related reference to check the concreted information on the catalyst and reaction conditions.

**Table 4**  
Catalytic epoxidation of different olefins over  $\text{PMo}_{11}\text{Co}/\text{SBA}$  catalyst with  $\text{O}_2/\text{IBA}$ .<sup>a</sup>

Substrate	Time (h)	Conversion (%)	Selectivity (%)		Others (%)
			Epoxide	Others	
	7	93	>99	nd	
	1	89	7	77 (Pha) <sup>b</sup> 15 (Bza) <sup>c</sup>	
	0.3	39	65	34 (Ketone)	
	5	65	76	23 (Bza) <sup>c</sup>	

<sup>a</sup> Reaction conditions: catalyst 10 mg, olefin 1.0 mmol,  $\text{CH}_3\text{CN}$  10 ml, flow of air 10 ml/min, IBA 2.0 mmol, reaction temperature 40 °C.

<sup>b</sup> Phenylacetaldehyde.

<sup>c</sup> Benzaldehyde.

(90% of epoxide selectivity). Notably, the epoxidizing selectivity of these two catalysts are equivalent to the montmorillonite supported cobalt porphyrin catalyst ( $\text{CoTE3PyP/MT}$ ) and the Ga-based metal-organic framework (MOF) supported copper catalyst ( $\text{Cu@COMOC-4}$ ) [21,23], and much higher than other Co-based catalysts like  $\text{Co/ZIF}$  and cobalt phosphonate-based MOF [14,19].

Moreover, the catalyst  $\text{PMo}_{11}\text{Co/SBA}$  was also used to catalyze the epoxidation of other olefins with  $\text{O}_2/\text{IBA}$ . As shown in Table 4, the relatively inert terminal olefin of 1-octene can also be converted to epoxide rapidly, and a 98% conversion of 1-octene with nearly 100% selectivity of epoxide is achieved after 3 h. Besides,  $\text{PMo}_{11}\text{Co/SBA}$  is also active for the epoxidation of styrene,  $\alpha$ -methyl styrene and trans-stilbene. However, relatively low epoxidizing selectivity can be detected for these reactions. In these cases, aldehyde or ketone turns to the main product, and very high selectivity to phenylacetaldehyde (77%) can be obtained for the oxidation of styrene.

#### 4. Conclusions

In summary, hybrid heterogeneous catalysts for aerobic epoxidation of olefins can be obtained by immobilizing transition metal-substituted phosphomolybdic acids ( $\text{PMo}_{11}\text{M}$ ,  $\text{M} = \text{Fe}, \text{Co}, \text{Cu}$ ) on amino-functionalized SBA-15. The SBA-15 supported  $\text{PMo}_{11}\text{Co}$  catalyst exhibits relatively high catalytic activity and selectivity for the epoxidation of cyclooctene, cyclohexene and 1-octene with  $\text{O}_2$  as oxidant and IBA as co-reagent. Selecting suitable solvent of acetonitrile can inhibit the deactivation of the catalyst, which can significantly improve the recyclability and stability of the SBA-15 supported  $\text{PMo}_{11}\text{Co}$  catalyst.

#### Acknowledgment

Financial support from the National Natural Science Foundation of China (No. 21173100 and 21320102001) is gratefully acknowledged.

#### References

- [1] P. Cancino, V. Paredes-García, P. Aguirre, E. Spodine, *Catal. Sci. Technol.* 4 (2014) 2599–2607.
- [2] J.R. Monnier, *Appl. Catal. A: Gen.* 221 (2001) 73–91.
- [3] S.R. De, G. Kumar, J.L. Jat, S. Birudaraju, B. Lu, R. Manne, N. Puli, A.M. Adebesin, J.R. Falck, *J. Org. Chem.* 79 (2014) 10323–10333.
- [4] J. Song, Z. Zhang, T. Jiang, S. Hu, W. Li, Y. Xie, B. Han, *J. Mol. Catal. A: Chem.* 279 (2008) 235–238.
- [5] S. Pathan, A. Patel, *Chem. Eng. J.* 243 (2014) 183–191.
- [6] N. O'Callaghan, J.A. Sullivan, *Appl. Catal. B: Env.* 146 (2014) 258–266.
- [7] S.D. Bishopp, J.L. Scott, L. Torrente-Murciano, *Green Chem.* 16 (2014) 3281–3285.
- [8] T. Mukaiyama, T. Yamada, T. Nagata, K. Imagawa, *Chem. Lett.* (1993) 327–330.
- [9] T. Nagata, K. Imagawa, T. Yamada, T. Mukaiyama, *Chem. Lett.* (1994) 1259–1262.
- [10] T. Punniyamurthy, B. Bhatia, M.M. Reddy, G.C. Maikap, J. Iqbal, *Tetrahedron Lett.* 53 (1997) 7649–7670.
- [11] X. Zhou, Q. Tang, H. Ji, *Tetrahedron Lett.* 50 (2009) 6601–6605.
- [12] W. Nam, S.J. Baek, K.A. Lee, B.T. Ahn, J.G. Muller, C.J. Burrows, J.S. Valentine, *Inorg. Chem.* 35 (1996) 6632–6633.
- [13] X. Zhou, H. Ji, *Chem. Eng. J.* 156 (2010) 411–417.
- [14] A. Zhang, L. Li, J. Li, Y. Zhang, S. Gao, *Catal. Commun.* 12 (2011) 1183–1187.
- [15] M.E. Nino, S.A. Giraldo, E.A. Páez-Mozo, *J. Mol. Catal. A: Chem.* 175 (2001) 139–151.
- [16] Z. Li, H. Ding, S. Wu, H. Liu, H. Su, J. Sun, D. Zheng, Q. Huo, J. Guan, Q. Kan, *Mater. Res. Bull.* 48 (2013) 1920–1926.
- [17] M. Chibwe, T.J. Pinnavaia, *J. Chem. Soc. Chem. Commun.* (1993) 278–280.
- [18] J.H. Schutten, *Makromol. Chem.* 180 (1979) 2341–2350.
- [19] R. Sen, D. Saha, D. Mal, P. Brandão, G. Rogez, Z. Lin, *Eur. J. Inorg. Chem.* (2013) 5020–5026.
- [20] E. Angelescu, R. Ionescu, O.D. Pavel, R. Zăvoianu, R. Birjega, C.R. Luculescu, M. Florea, R. Olar, *J. Mol. Catal. A: Chem.* 315 (2010) 178–186.
- [21] H. Kameyama, F. Narumi, T. Hattori, H. Kameyama, *J. Mol. Catal. A: Chem.* 258 (2006) 172–177.
- [22] S. Lim, M. Kang, J. Kim, I. Lee, *Bull. Korean Chem. Soc.* 26 (2005) 887–890.
- [23] Y. Liu, K. Leus, T. Bogaerts, K. Hemelsoet, E. Bruneel, V. Van Speybroeck, P. Voort, *ChemCatChem* 5 (2013) 3657–3664.
- [24] B.J.S. Johnson, A. Stein, *Inorg. Chem.* 40 (2001) 801–808.
- [25] N. Maksimchuk, M. Melgunov, Y. Chesarov, J. Mrowiecblalon, A. Jarzebski, O. Kholdeeva, *J. Catal.* 246 (2007) 241–248.
- [26] J. Gamelas, D. Evtuguin, A. Esculcas, *Transition Met. Chem.* 32 (2007) 1061–1067.
- [27] N. Mizuno, M. Misono, *Chem. Rev.* 98 (1998) 199–217.
- [28] R. Neumann, A. Khenkin, *Chem. Commun.* (2006) 2529–2538.
- [29] A. Haimov, R. Neumann, *Chem. Commun.* (2002) 876–877.
- [30] R. Neumann, H. Miller, *J. Chem. Soc. Chem. Commun.* (1995) 2277–2278.
- [31] Z. Olejniczak, B. Sulikowski, A. Kubacka, M. Gasior, *Top. Catal.* 11/12 (2000) 391–400.
- [32] S. Kasztelan, J.B. Moffat, *J. Catal.* 106 (1987) 512–524.
- [33] R. Fricke, G. Ohlmann, *J. Chem. Soc. Faraday Trans. I* 82 (1986) 273–280.
- [34] K. Bruckman, M. Che, J. Haber, J.M. Tatibouet, *Catal. Lett.* 25 (1994) 225–240.
- [35] J.B. Moffat, S. Kasztelan, *J. Catal.* 109 (1988) 206–211.
- [36] A.C. Estrada, I. Santos, M. Simões, M. Neves, J. Cavaleiro, A. Cavaleiro, *Appl. Catal. A: Gen.* 392 (2011) 28–35.
- [37] L. Hua, Y. Qiao, Y. Yu, W. Zhu, T. Cao, Y. Shi, H. Li, B. Feng, Z. Hou, *New J. Chem.* 35 (2011) 1836–1841.
- [38] J. Du, J. Yu, J. Tang, J. Wang, W. Zhang, W.R. Thiel, M. Jia, *Eur. J. Inorg. Chem.* (2011) 2361–2365.
- [39] H. Gao, J. Yu, J. Du, H. Niu, J. Wang, X. Song, W. Zhang, M. Jia, *J. Clust. Sci.* 25 (2014) 1263–1272.
- [40] J. Wang, Y. Zou, Y. Sun, M. Hemgesberg, D. Schaffner, H. Gao, X. Song, W. Zhang, M. Jia, W.R. Thiel, *Chin. J. Catal.* 35 (2014) 532–539.
- [41] K. Li, J. Wang, Y. Zou, X. Song, H. Gao, W. Zhu, W. Zhang, J. Yu, M. Jia, *Appl. Catal. A: Gen.* 482 (2014) 84–91.
- [42] B. George, A. Tsigdinos, C. Hallada, *Inorg. Chem.* 7 (1968) 437–441.
- [43] D. Zhao, Q. Huo, J. Feng, B.F. Chmelka, G.D. Stucky, *J. Am. Chem. Soc.* 120 (1998) 6024–6036.
- [44] H. Wang, J. Huang, S. Wu, C. Xu, L. Xing, L. Xu, Q. Kan, *Mater. Lett.* 60 (2006) 2662–2665.
- [45] A. Patel, S. Pathan, *J. Coord. Chem.* 65 (2012) 3122–3132.
- [46] B. Sulikowski, R. Rachwalik, *Appl. Catal. A: Gen.* 256 (2003) 173–182.
- [47] M. Nakayama, T. Ii, K. Ogura, *J. Mater. Res.* 18 (2003) 2509–2514.
- [48] A.M. Khenkin, A. Rosenberger, R. Neumann, *J. Catal.* 182 (1999) 82–91.
- [49] O. Kholdeeva, M. Vanina, M. Timofeeva, R. Maksimovskaya, T. Trubitsina, C. Hill, *J. Catal.* 226 (2004) 363–371.